Stresses in sand casting – Analysis and optimized solutions for improved casting designs and product quality

Sand casting of metal parts is one of the most flexible manufacturing processes for differently shaped and sized castings. The process is applicable for a wide range of alloys and the obtained material quality and dimensional tolerances can be controlled by modifying either the design of the part or the casting layout. The flexibility in design provided by the shaping sand material and the internal sand cores often leads to a complex cooling history, which highly affects the evolution of properties and defects. Many defects in the final part like e. g. cold cracks and hot tears are related to the stresses that build up during cooling. This article presents how MAGMASOFT® is used to analyze and optimize both the casting design and the casting process by combining the thermal analysis of the casting process with an integrated prediction of stress and distortion. It is shown how the thermal gradients, cooling time and constraints from the mold and core materials affect the risk of stress related defects and unwanted distortion. Methodological application on industrial examples show the significant advantages of being able to systematically analyze different designs and casting layouts upfront, to avoid quality problems in production and fulfill dimensional tolerance requirements.

Jesper Thorborg, Jörg Zimmermann and Corinna Thomser, Aachen

1 Introduction – Stress simulation in sand casting

When liquid metal is poured into the cavity of the mold, the sand starts to heat up while the liquid metal cools and solidifies. Thermal contraction of the metal and thermal expansion of the sand influence the initial location of the interface between the solidifying metal and the surrounding sand mold and the inner cores, which governs the initial shape of the cast part. During the subsequent solid state cooling, the cast material gains strength compared to the sand and further contraction is mainly governed by the thermal gradients in the metal. Generally, the outer regions and thinner sections cool first and due to the related thermal contraction, these regions build up tensile stresses. The outer tensile stresses are in balance with the inner still hotter regions, where mainly compressive stresses build up. Due to the initial compression of the inner and weaker material, the sign of the stress state changes during further cooling. This means at room temperature the outer surface is typically in compression. The change in stress state during cooling is illustrated by the simulation results in **Figure 1**.

At high and intermediate temperature levels the metal is vulnerable to form defects which are related to high stresses and inelastic deformation e. g. localizing around porosity. For hot tearing, the risk and level of defects are closely related to the complex balance between sufficient feeding of solidifying regions to compensate for contraction and the level of constraints from e. g. cores that prevents the cast material to contract freely. At temperature levels below solidus, uneven cooling leads to different levels of contraction which can promote high stress levels. In some cases, the high stress level leads to permanent deformation that affects the dimensions of the final part, and in worse cases the stress level reaches the strength of the material and cracks can start to form. Depending on the size of the casting, time can have an important in-

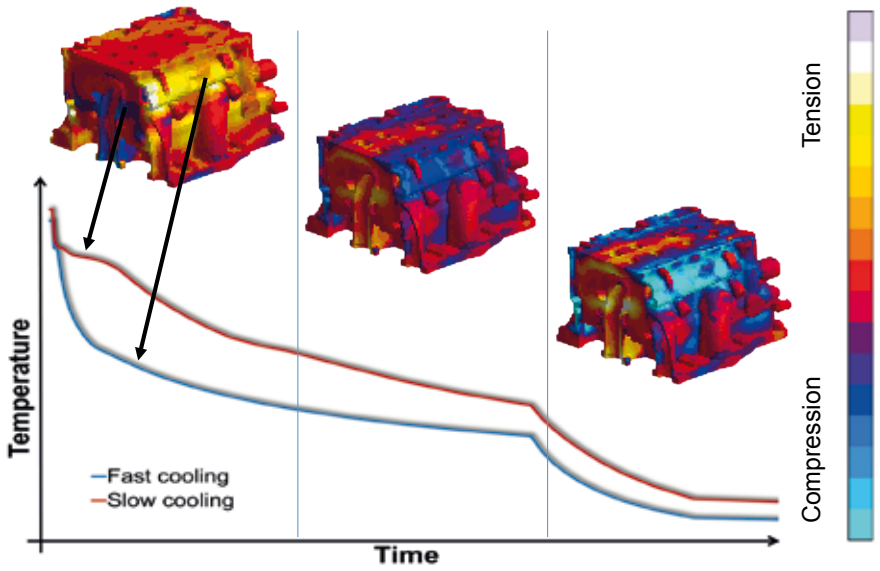

Figure 1:
Thermal history and related stress evolution in castings. Faster cooling results in transient tensile stresses on the surface followed by compression at room temperature due to initial permanent deformation in the hotter inner regions.

PHOTOS AND GRAPHICS SOURCE: MAGMA

fluence on the stress evolution during solidification and cooling, [1, 2]. For large sized castings, the cooling time is typically large enough to allow stress relaxation to take place. Similar to stress relaxation during heat treatment, this is governed by creep and visco-plastic material behavior, [3, 4].

In **Figure 2**, six different cases are presented, describing the analysis and benefits from stress simulations for different applications.

2 Stress predictions in large castings – Validation

Casting of large scale steel and iron parts leads to long solidification and cooling times. Stress simulations of these castings have to take the time scale of the process into account to properly predict stress relaxation at high temperatures. For these types of cases, a unified creep model is used to include both temperature and time dependency in the model description. Including time dependency in the material model description allows the simulation to predict the transient and residual stress levels with a reasonable accuracy, as shown in the examples in this section where simulation results are compared to stress measurements, [5].

MAN Energy Solutions designs large two stroke marine engines, where roughly 1/3 of the modern large-bore diesel engine is made of cast components. The company decided to closely investigate the residual stress state in the cylinder frames, by measuring the residual stresses after the casting process and comparing the stress level to simulation results. After careful evaluation, the ring core method was determined to be suitable measuring the stress level for cast iron parts. The full casting process was simulated using MAGMASOFT® including the simulation of stresses and deformation, [A].

The ring core method works by releasing the stress state in a small stub of material, by milling a small notch around a rosette of strain gauges. During milling the strains are measured in the rosette and are converted to stresses as a function of the depth of the notch[1]. See the assembled engine, the measurement setup and details about the notch and rosette in **Figure 3**.

Mechanically loaded grey iron bars with well defined boundary conditions were used for evaluating the method. The objectives were to gain confidence in the method and ensure successful application on different iron grades. The ring core method was also simulated during validation, and the stress release after milling the notch was very nicely shown in the stress lattice example in **Figure 4**. In Figure 4a the material was initially loaded in tension in the middle of the bar, but during milling the notch, the stress state redistributed and after a few milimeters it dropped to approximately zero (Figure 4b).

For the real casting measurements, three cylinder frames were selected. One 20 ton grey iron frame and two ductile iron frames of 10 and 25 tons, respectively.

The first set of measurements was done on the 20 ton grey iron frame. The location of the measurements was a number of supporting bars, which were part of the casting layout but were removed before machining. Unfortunately, some large stress gradients, which were later seen in the simulation, turned out to cause problems for the measurements. The comparison to simulation results showed similar trends but quite some differences in the absolute values and results, see **Figure 5**.

Based on the experience from the grey iron frame, it was decided to simulate the casting process first to get an overview of the residual stress state in the material, before doing the measurements. Critical areas with plateaus of either compressive or tensile stress states were selected for measurements before doing the actual stress measurements at the foundries.

The small ductile iron frame was subsequently evaluated. For this frame, the thermal results were used to perform two stress simulations. One simulation used the standard time independent plasticity model and one used the unified creep model to evaluate the influence of stress relaxation at the higher temperature levels. The simulated results showed a clear tendency

[1] In this way the ring core method resembles the more well-known hole drilling method, where the stress state is also measured by releasing the stress state during drilling.

Stress predictions in large castings – Validation

Example: Large ductile iron and grey iron 2-stroke marine cylinder frames

- Stress simulation results were compared to measurements, using the ring core method
- The influence of time and stress relaxation was evaluated, using the unified creep model

Fulfill dimensional requirements – Flatness and roundness

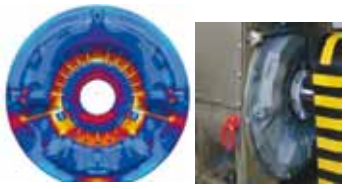

Example: Cast iron electric engine cover

- Flatness and roundness were evaluated and compared for both simulation results and measurements
- The stress level was shown to not be critical and it was possible to save an expensive stress relief heat treatment step

Minimizing the risk of hot tearing – using virtual Design of Experiments (DoE)

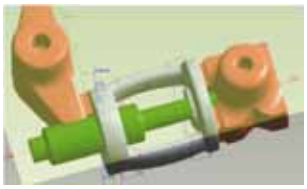

Example: Crucial part of a pump assembly

- The risk of hot tears and shrinkage porosity was evaluated in four critical areas
- Virtual DoE was used to evaluate the influence of feeder layout, the part design and process conditions

Risk of cracks during machining

Example: Cast iron frame structure

- Stress redistribution due to machining was evaluated
- Uncritical residual stress levels after casting were shown to increase and provoke cracks during machining
- The influence of changing the casting layout and cooling conditions were evaluated

Optimization of quench conditions

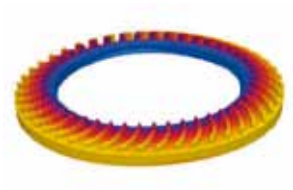

Example: Steel brake disc

- Simulation of distortion of steel brake discs during quenching
- Different quench conditions were simulated to analyze the influence of stacking the discs during quenching
- Both oil and water were considered as quench media

Integrated distortion control in casting and heat treatment

Example: Steel blade for a Francis turbine

- Simulation of the contraction and deformation during cooling was used to pre-shape the mold to get agreement with the target geometry
- Stresses and deformation in the heat treatment support frame were evaluated
- 3D measurements were compared to simulation results

Figure 2: Six different cases, describing the analysis and benefits from stress simulations for different applications.

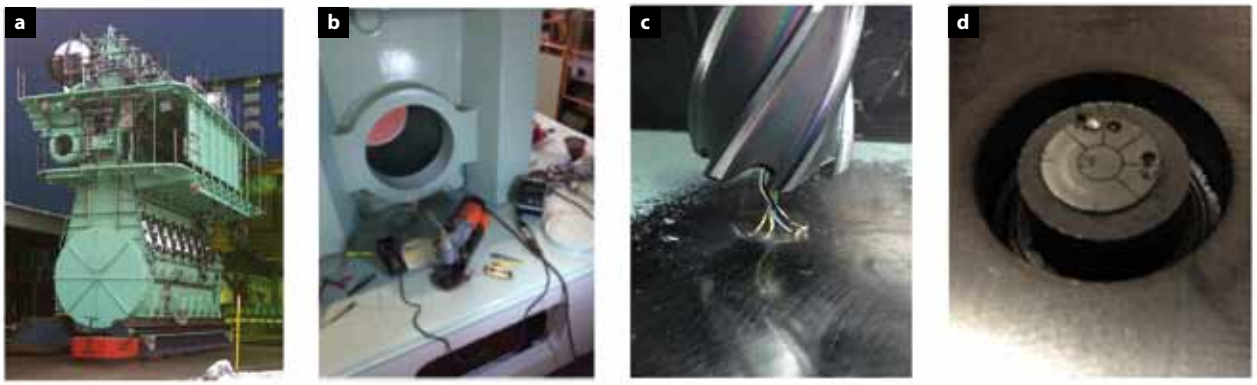

Figure 3: Determination of stress levels for a large, two-stroke marine diesel engine (a), handheld ring core measurement equipment (b) and zoom of drill and mounted strain gauge (c, d).

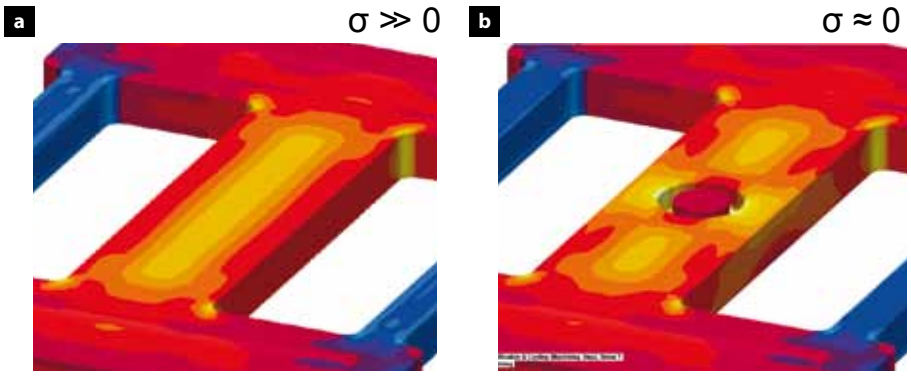

Figure 4:
Illustration of the simulated stress state in a stress lattice (a) and predicted stress release simulating the ring core method (b).

Figure 5: Stress measurements for a 20 ton grey iron casting, with 9 successful measurements (a) and measurements compared to simulation results (b).

of lower residual stresses when stress relaxation was taken into account by the unified creep model, see **Figure 6**.

Measurements were subsequently performed and compared to the results from the two simulations. The comparison was very convincing. Generally, the results from both simulations followed the trends from the measurements, but the results from the unified creep simulation showed a much better agreement in the stress level compared to the simulation where the plasticity formulation was used. This showed the expected need for time dependency to be included in the material description to simulate stress relaxation at high temperature levels. Measurement and simulation results of the larger 25 ton ductile iron casting showed similar good agreement. Again, the trends were similar for the two material models, but the results using the unified creep model showed best agreement.

Generally, the ring core method proved to be a viable measurement method for the large cast iron cylinder frames. The method showed some sensitivity to the preparation of the test

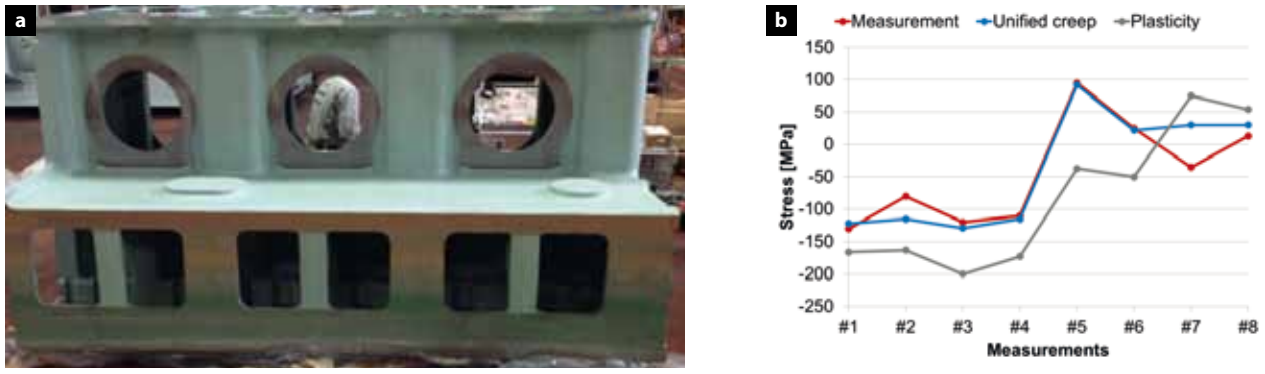

Figure 6: 10 ton ductile iron casting, with 8 successful measurements (a) and measurements compared to simulation (b).

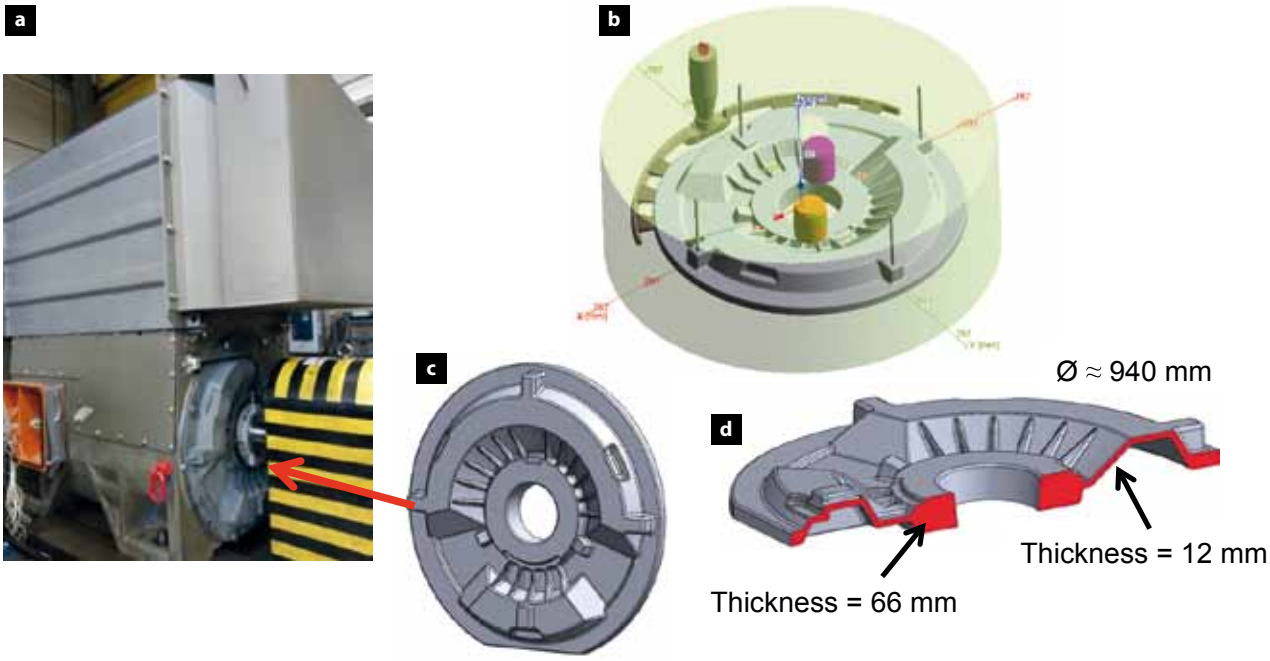

Figure 7: Snapshot of the mounted engine cover (a), casting design used in the simulation (b), closeup of the engine cover (c) and cross section (d).

area, due to grinding the surface and gluing the strain gauge rosette onto the surface. As expected, the measurements were sensitive to the location on the frame, especially if some larger stress gradients are expected in the area.

Overall, the agreement between measurements and simulation results was quite good and the unified creep model was able to take the stress relaxation, which takes place in the large slow cooling cylinder frames, into account.

3 Fulfill dimensional requirements – Flatness and roundness

When cast components fail or cause problems under service load conditions, it is typically necessary to perform a thorough review of the entire process chain starting with the casting process. Similar to the design phase and process optimization phase, it is important to have a simulation strategy to review and analyze the conditions in the process and the material. In this section, a cast iron electric engine cover showed vibration problems during testing of the prototype parts. This could finally lead to premature failure. Initial tests showed that after a stress relief treatment the engine vibration problem was reduced, suggesting a problem of dimensional stability and the presence of residual stresses. It was decided to evaluate the influence of residual stresses on the distortion, which was assumed to cause the dimensional requirement problem initially, [B].

Deformation was measured and simulated in order to evaluate the two criteria of flatness and roundness. The evaluation

was finally used to conclude whether the stress relief heat treatment after casting was necessary. The engine cover and the details regarding dimensions and location in the assembly are shown in **Figure 7**.

The evaluation of the dimensional requirements was done across all manufacturing steps. The roundness was evaluated around the bearing and the flatness was evaluated on both the back face of the cover and on both sides of the bearing face, (details about the different locations of evaluation in **Figure 8**). The arrow A indicates the location of roundness and the arrows B, C and D indicate the location of flatness evaluation.

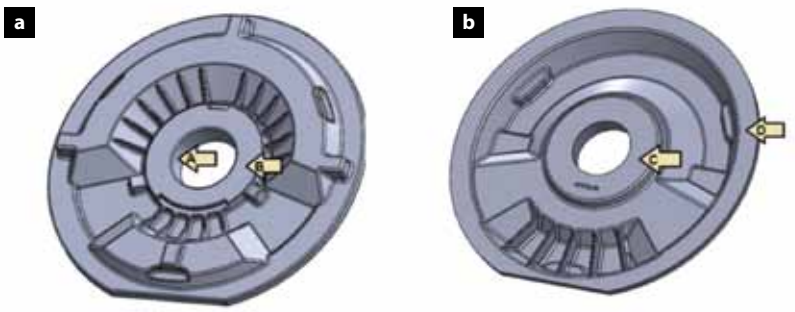

Figure 8: Location of roundness and flatness evaluations at the front face (a) and back face (b). The arrow A indicates the location of roundness evaluation and arrows B, C and D indicate the locations of flatness evaluation.

A full casting process simulation was performed and the stress state was evaluated after the casting process using MAGMASOFT®. The von Mises result showed some high stress levels around the ribs on both sides of the cover, indicating that the cooling history did generate some permanent deformation at high temperature, which could lead to critical levels of distortion. The von Mises stress level is shown in **Figure 9** on both sides of the cover.

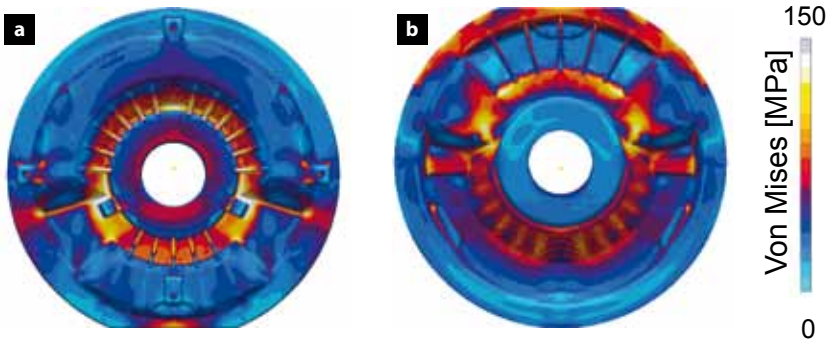

Figure 9: Von Mises stress level after the casting process, showing high stresses around the ribs.

The displacement results showed some tendency to bending, which is visualized by the z-displacement result in **Figure 10**. This result shows that the part did not only contract due to cooling, but as indicated by the residual stress result, it also distorted in terms of bending.

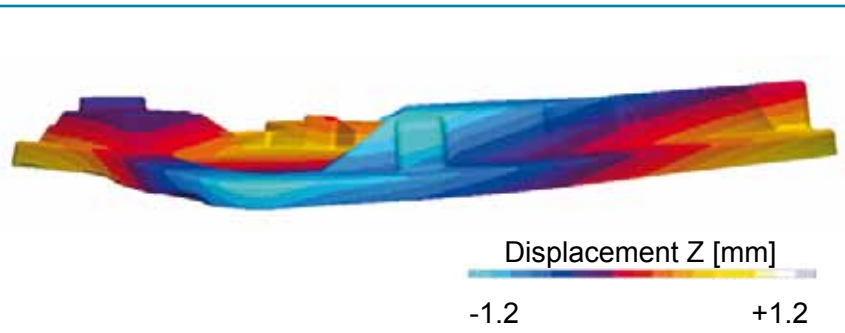

Figure 10: Displacement Z result after casting, indicating bending of the cover.

The simulation results were compared to measurements by positioning the geometry using the 6-points measurement method to overlay the results. The measurements were done on 50 points around the perimeter of the different evaluation areas.

The comparison was done by visualizing the measurements and simulation results in both a polar plot and in a classical xy-graph. The polar plot fits well to the round geometry and represents well the evaluation around the perimeter. An example is shown in **Figure 11** for the outer flange.

Generally, the comparison on the outer flange showed a quite good agreement between simulation and measurements.

The roundness of the part was evaluated in the inner perimeter of the flange by calculating the distances between the measurement points and an evaluation circle. The radius of the evaluation circle is constructed by the least square method to minimize the deviation between the measurements and the circle. In addition to the individual comparison in the points on the perimeter, the roundness was evaluated by the difference between the minimum and maximum values shown as ΔZq in **Figure 12**a. The overall roundness is visualized in the two graphs, Figure 12b and Figure 12c.

The comparison showed good agreement between the different measurements, and the comparison to the simulation results showed agreement within the specified tolerances. The roundness number ΔZq was 0.276 mm and 0.339 mm for the two measurements and 0.9 mm for the simulation results. The

higher value found by the simulation result is partially due to the slaut evaluation surface, which made it hard to compare the roundness at the exact same diameter. Further comparison was done after the stress relief heat treatment and a similar agreement was found for the roundness evaluation, with a slight decrease in the ΔZq number to 0.222 mm.

Overall the evaluation of both the flatness and roundness criteria showed good and consistent agreement between measurements and simulation results. The presented approached was capable to give a successful dimensional evaluation. Based on the results it was possible to conclude that the observed problem of vibrations was not related to the casting process. It was furthermore shown that the stress relief heat treatment step was not necessary, since the residual stresses did not affect the roundness of the hub, and it was decided to skip the heat treatment step and by that save 13,000 US$/year.

The original vibration problem was subsequently further analyzed and solved by the R&D team, without modifying the casting process.

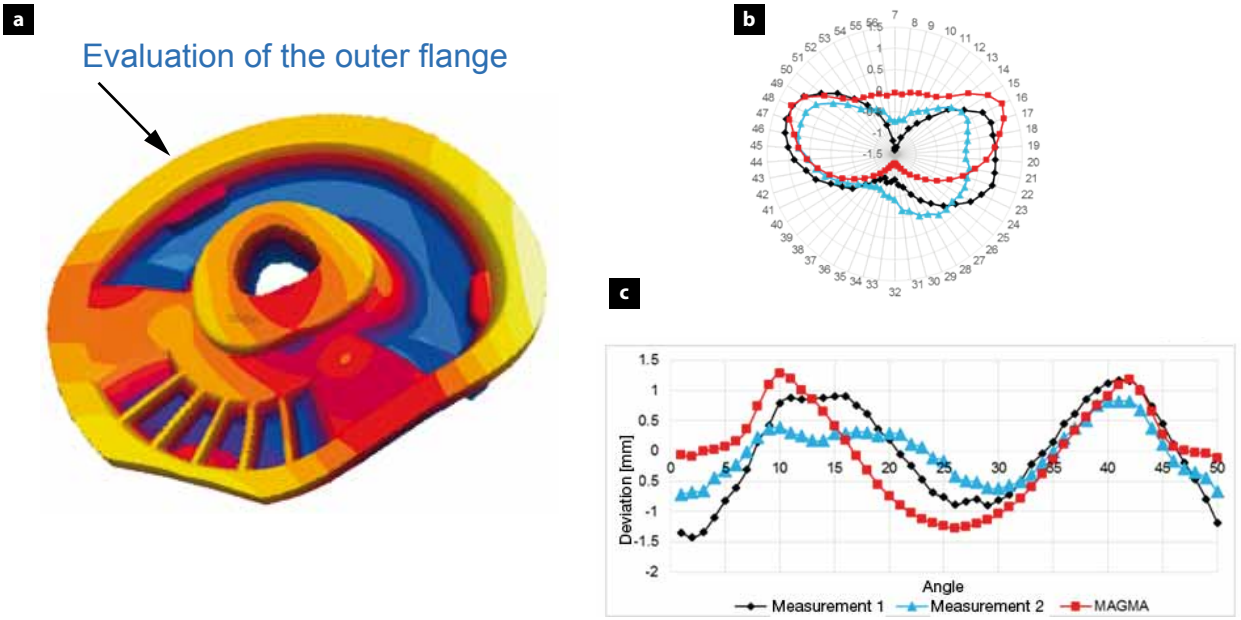

Figure 11: Evaluation of the distortion in the outer flange.
The simulated deformation result shown with 10x magnification (a), the comparison in polar plot (b) and in a xy-graph (c).

Figure 12: Roundness evaluation using the evaluation circle (a), comparison around the perimeter (b) and comparison in a xy-graph (c).

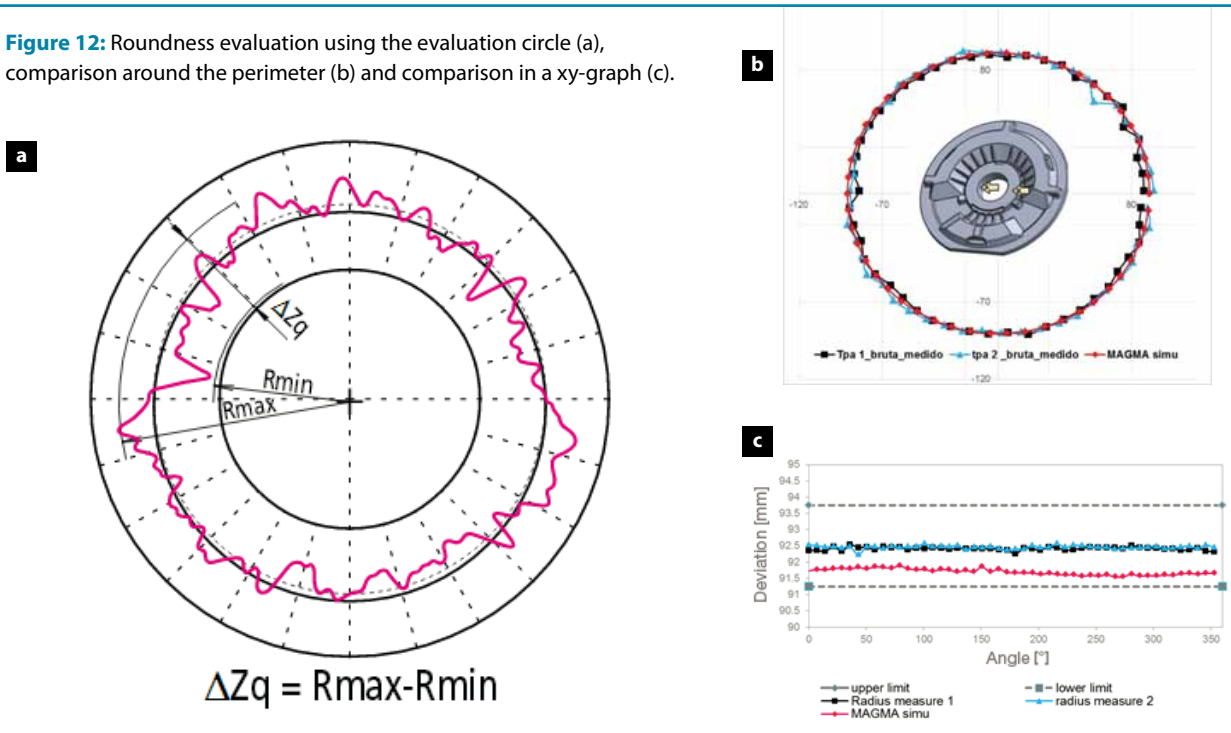

4 Stress related casting defects

Hot tearing of steel castings is a prime concern for foundries, which adds extra costs and time in the production in terms of repair welding and in the worst case high scrap rates. Thermal analysis of the casting process increases the understanding of the cooling conditions in critical areas, highlighting the risk of porosity formation, hot spots with poor or no feeding, and variations in cooling rates which governs the thermal contraction of the material. Based on the thermal analysis it is possible to extend the knowledge by coupling the results to a stress calculation, which provides information about thermal contraction. Critical areas can then be detected, if large strain rates and strain localize in hot spots where porosity already exists due to poor feeding.

To aid the foundry engineer identifying these critical areas prior to production, information from the thermal and mechanical analysis has been combined into a hot tear criterion, which highlights the critical areas directly as one result. The criterion takes various information into account to evaluate the complex physics that cause hot tearing.

To illustrate the application of the hot tear criterion on a real casting, an example is shown in **Figure 13**. The cracked zone is highlighted in Figure 13a and the predicted locations are indicated with yellow and red colors by the hot tear result in Figure 13b. In this case a long narrow feeding path was the root cause for hot tearing, and with the hot tear criterion it was possible to optimize the location and size of the feeders to minimize the hot tear problem sufficiently.

5 Minimizing the risk of hot tearing – using virtual DoE

To reduce and avoid the extra cost of repair welding of hot tears, it is beneficial to evaluated and review the risk of hot tears in a systematic way to select the best possible design and process conditions. The considered example in this section is called the Yoke, which is a crucial part of a pump assembly. The initial design and layout of the feeders produced close to 80 % scrap, due to hot tears in the inner corners of the longitudinal braces, see **Figure 14** where one of the locations is highlighted. The hot tears required extensive re-work, including repair welding of the defect locations. In addition, it was necessary to carry out a magnetic particle inspection to check all of the produced castings. As a result, the cost to produce this casting using the existing tooling was not favorable.

The foundry concluded that, in order to optimize production, it was necessary to work out and verify changes both in the part design and in the gating and feeding system of the casting. To tackle this task time- and cost-effectively, the approach to the problem chosen was to carry out a virtual Design of Experiments to evaluate different combinations of the design changes [C].

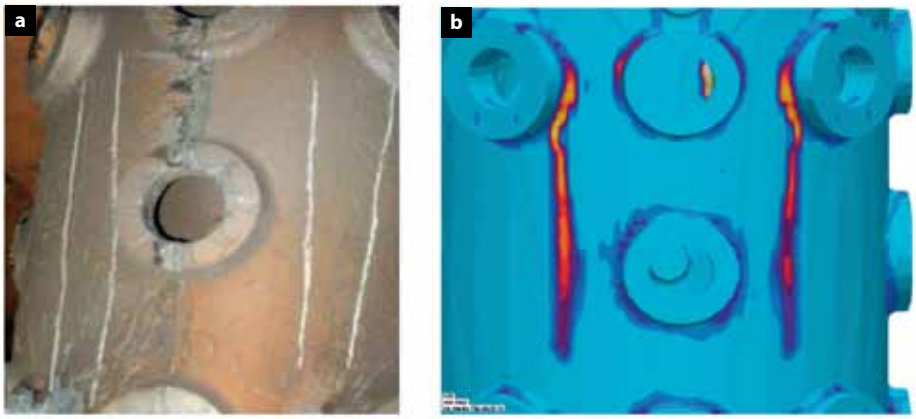

Figure 13:
Location (a) and prediction (b) of hot tears on a large steel casting.

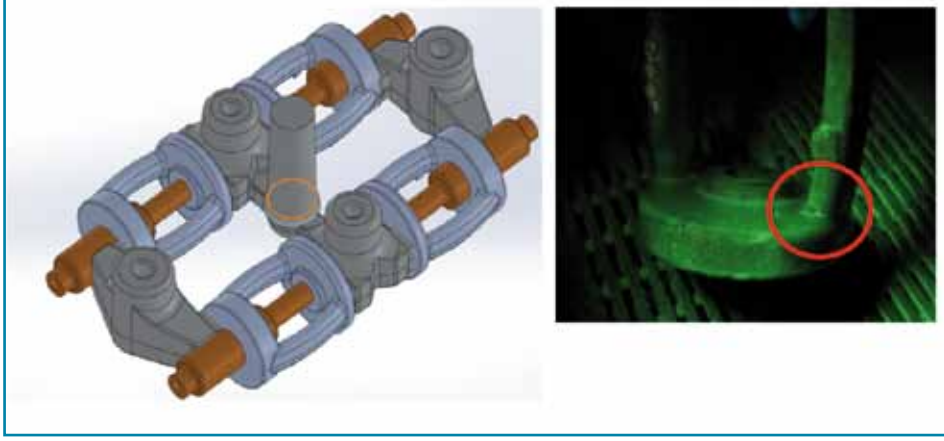

Figure 14:
Original situation: CAD model of the casting and the problem area.

To evaluate the designs, the four inner corners were identified as the critical areas and four corresponding evaluation areas were defined. In these areas the objective to be fulfilled to find the best design was to minimize the hot tear criterion, as well as to minimize the porosity criterion to ensure the part would not suffer from larger shrinkage defects (**Figure 15**).

Twelve designs were evaluated, where the position of the casting, the casting geometry, the feeder configuration and the process parameters were modified. The evaluation of each design included a full thermal analysis providing information about the feeding, porosity level and temperature information for the subsequent stress analysis. The hot tear criterion was calculated during the stress calculation, and the combined information was examined in the previously defined critical areas (**Figure 16**).

For the optimization assessment, statistical tools were used to identify the best compromise between hot tear and porosity tendency in the designs. A bar chart displaying both defined objectives for each design clearly shows opposing trends regarding porosity and hot tearing (**Figure 17**).

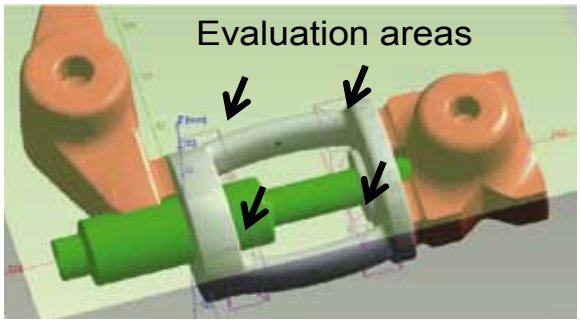

Figure 15: Definition of the evaluation areas for the analysis of hot tearing tendency.

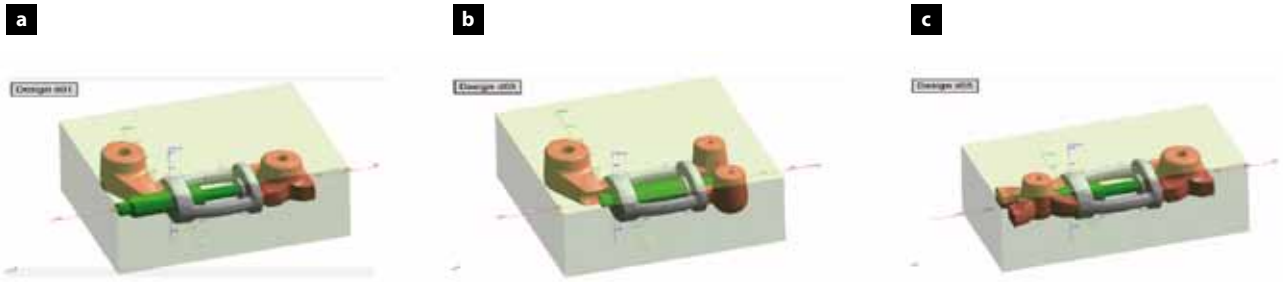

Figure 16: Different feeder configurations: three out of the 12 automatically simulated designs.

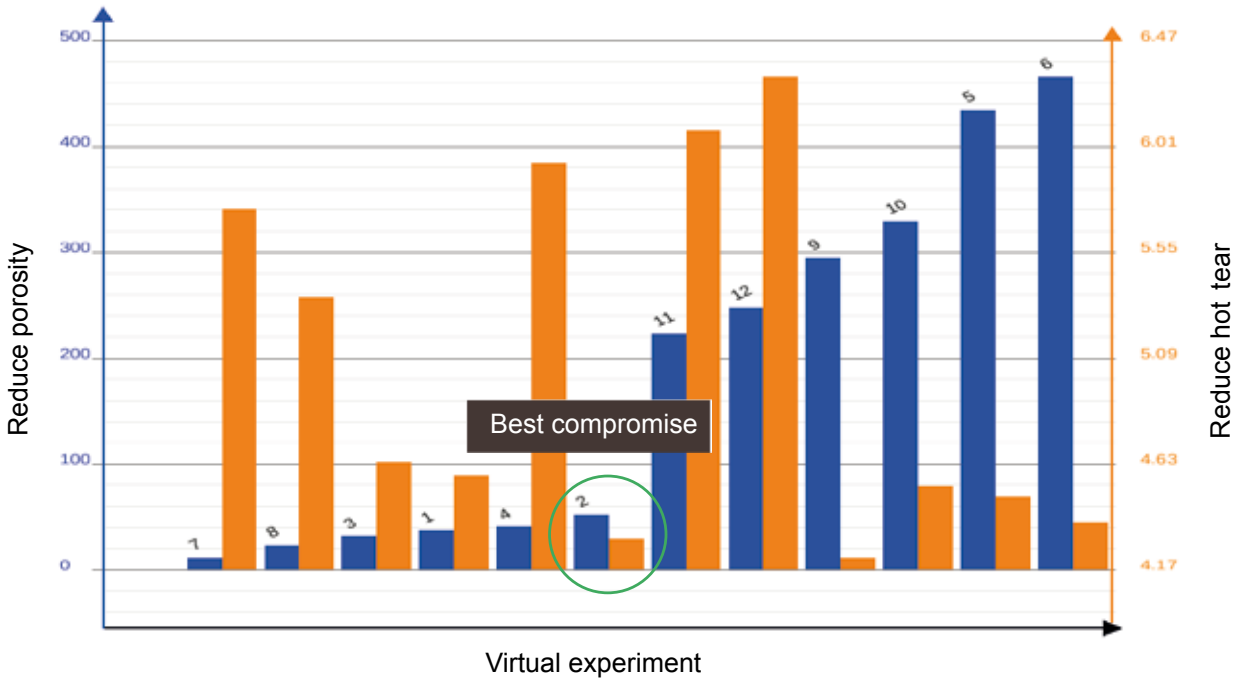

Figure 17: Porosity and related hot tear tendency for all virtual experiments in a bar chart representation. Design 2 provides the best compromise.

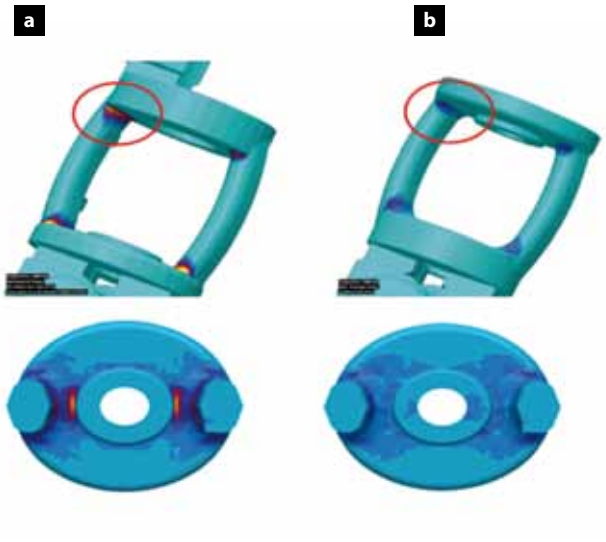

Figure 18: Indications of hot tearing in the original layout (a) and in the optimized design (b).

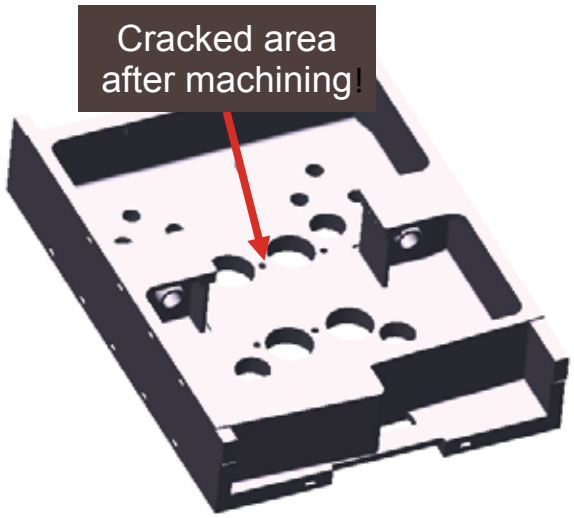

Figure 19: Geometry of the machined part, with critical area highlighted.

As expected, the strongest tendency for hot tearing was revealed for optimum feeding with minimum porosity. This is due to longer solidification times and increased temperature differences between the casting and the feeders, which promotes feeding, but also results in high strain rates and an increased tendency for hot tearing. The bar chart does however show a design that provides the best compromise between the two competing objectives.

A comparison of the results between the original situation and the best design considered in the optimization showed that geometric changes in both the casting and in the feeding system were necessary to significantly reduce both the stress and porosity defects at the same time (**Figure 18**).

Using the optimized solution, it was possible to reduce the hot tear risk in the critical solidification range by approximately 60 % compared to the original situation. The assessment tools allowed a quantitative comparison of how each design influenced each of the objectives. For the chosen solution, the changed feeder layout reduced the strain during solidification by 30 %, while the modified casting design reduced the strain during solidification by 44 %. It was subsequently possible to reduce both the amount of magnetic particle inspections required, as well as the amount of repair welding. The automatic calculation of the twelve versions was done on an 8-core workstation and took less than one day. To evaluate the designs in production would have taken weeks with high costs.

6 Risk of cracks during machining

Casting metal parts is often the first step in a sequence of downstream process steps which include cleaning, thermal treatment, machining, assembling etc. Most of these manufacturing steps affect the stress state in the material, either due to changes in microstructure and stress relaxation, or due to applied loads or removal of material.

To analyze the influence of downstream process steps on product quality it is often required to use the as-cast condition of the material as the starting point for the subsequent process step(s). In this section, the focus is on how the machining operations of two large holes and drilling of one additional hole influence the stress concentration in the remaining material between the holes. For this type of analysis, it is necessary to include the residual stress distribution from the casting process as initial condition for the subsequent removal of material. The example shows what a process engineer is typically able to change in the dimensions and casting layout to affect the cooling history, and by that improve the final quality and reduce the risk of cracks during machining.

The considered part is a large cast iron frame, with several holes in the base plate. The casting process showed no signs of problems both in reality and in simulated results. However, after machining the holes and drilling the center hole, cracks were detected in the material on the edge of the two holes, where the load carrying area was reduced and hence the stresses increased significantly (**Figure 19**).

The casting process was simulated with MAGMASOFT®. The thermal results showed a smooth cooling process with relatively small gradients througth the thickness of the walls but with a higher temperature level in the base plate compared to the surronding walls. The simulation predicted a moderate stress level in the base plate around the critial area, but not reaching a critical level for the GJL 200 material in the as-cast conditions, see **Figure 20**.

Results from simulating the machining operation, however, clearly showed an increase in the stress level in the critical area. The von Mises stress level increased from approximately 60 MPa to above 230 MPa, due to the reduction of the load carrying area by the machining operations.

Based on the initial analysis and the detected cracks on the real part, it was necessary to change the process and/or the design of the part to reduce the risk of cracks. The implemented changes had to be practically possible from a process point of view, the final part had to meet the design requirements, and finally the changes had to be cost effective.

For the considered problem mainly two things were interesting to be modified. First, the base plate was changed to reduce temperature differences to the surrounding walls, and thereby reduce the residual stress levels from the casting process. Second, the load carrying area between the two holes was increased. To modify the heat center in the base plate, it was decided to test two different approaches (**Figure 21**). In case 1, a chill was added next to the critical area to cool and strengthen the material locally during the casting process. In case 2, the holes in the base plate were filled with material to smoothen the temperature distribution during cooling. Finally, in case 3, material was added between the two holes in the

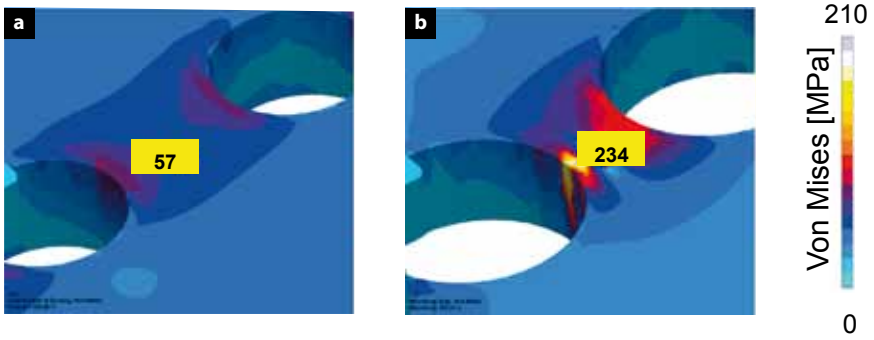

Figure 20:
Stress level in the critical area as-cast (a) and after machining (b), respectively.

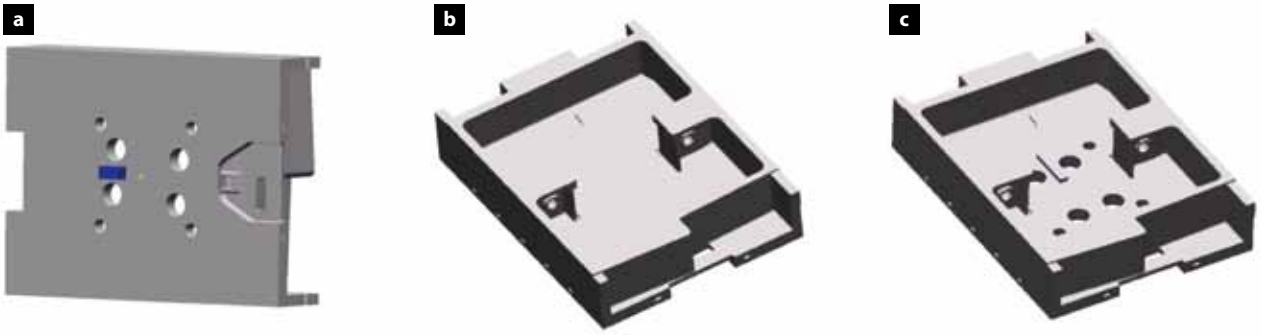

Figure 21: Evaluation of three different variants to reduce the risk of cracks in the critical area.

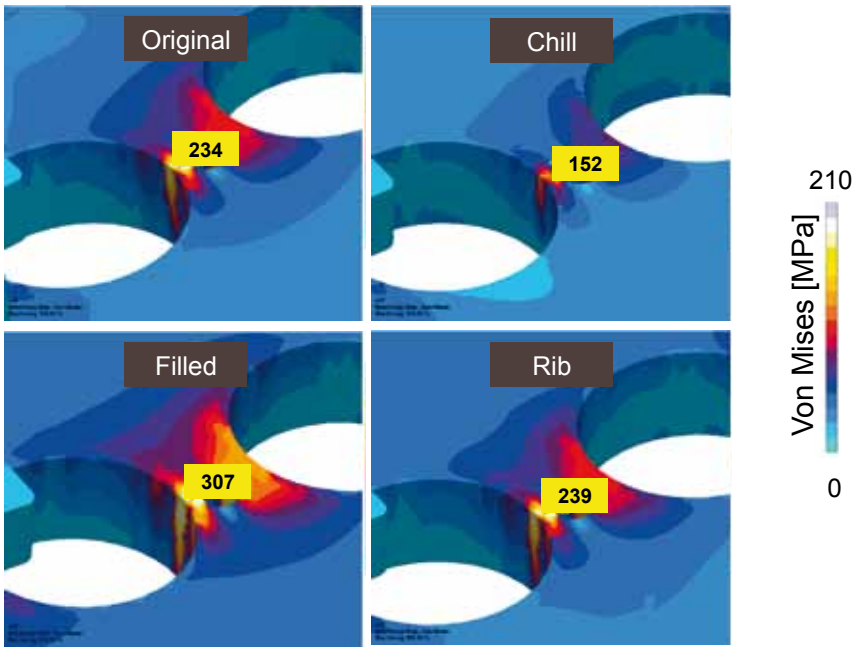

Figure 22:
Comparison of the results for the evaluated modifications after machining.

thickness direction of the base plate, to increase the load carrying area in the critical region.

The von Mises stress results for the 3 cases were compared to the original design after the machining step. Picked values in the critical region are shown in **Figure 22.**

The results showed a clear improvement in case 1, where the chill ensured a faster cooling of the critical area and by that locally reduced the level of residual stresses after the casting process and also significantly reduced the stress level after machining and drilling. Case 2, where the holes were filled with material, actually increases the problem. The extra material did locally smooth the temperature profile, but it also produced a bigger hot spot compared to the faster cooling walls. The residual stresses after casting therefore became bigger, which also increased the stress level in the critical area after machining. Finally, in case 3, no significant changes were observed and the added material between the two holes did not provide sufficient strength to solve the problem in the critical zone.

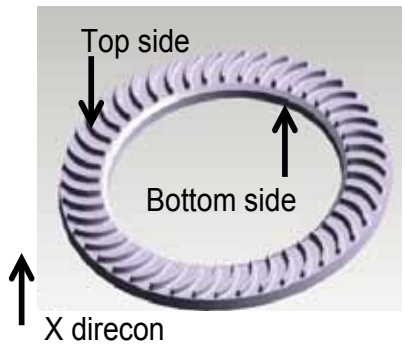

Figure 23: Geometry of the brake disc with inner diameter of 800 mm.

7 Optimization of quench conditions

Many cast components are heat treated after casting to release stresses built up during solidification and cooling and/or with the goal of changing the microstructure to obtain the required mechanical properties and performance. Especially during quenching of a casting, where uneven cooling rates due to different wall thicknesses or the quenching process itself occur, significant residual stresses and distortion can be introduced into the cast part. Distortion of steel brake discs during quenching plays a significant role in meeting the final dimensional requirements. In the case study shown here, the influence of various quench conditions was used with the optimization objective to minimize the distortion at the end of the quenching process. The geometry of the brake disc is shown in **Figure 23**. The calculations were done for low alloyed carbon steel with 0.25 % carbon (GS25Mn5). The material data were calculated with the thermodynamic software JMatPro version 8.0 (General Steel module).

The heat treatment module in MAGMASOFT® was used to calculate the quenching process, starting from 900 °C after the austenitization process. The discs were assumed stress free with no deformation at the beginning of quenching, i. e. the compared distortions were based on the different simulated quench temperatures only.

It is usually a big challenge to minimize distortion during quenching, due to the stacking of the brake discs. Depending on the location of the discs in the frame, some inner zones are quenched slower compared to outer zones which are quenched faster.

Displacement results for different water and oil quenching conditions are presented in **Figure 24**. Both homogeneous

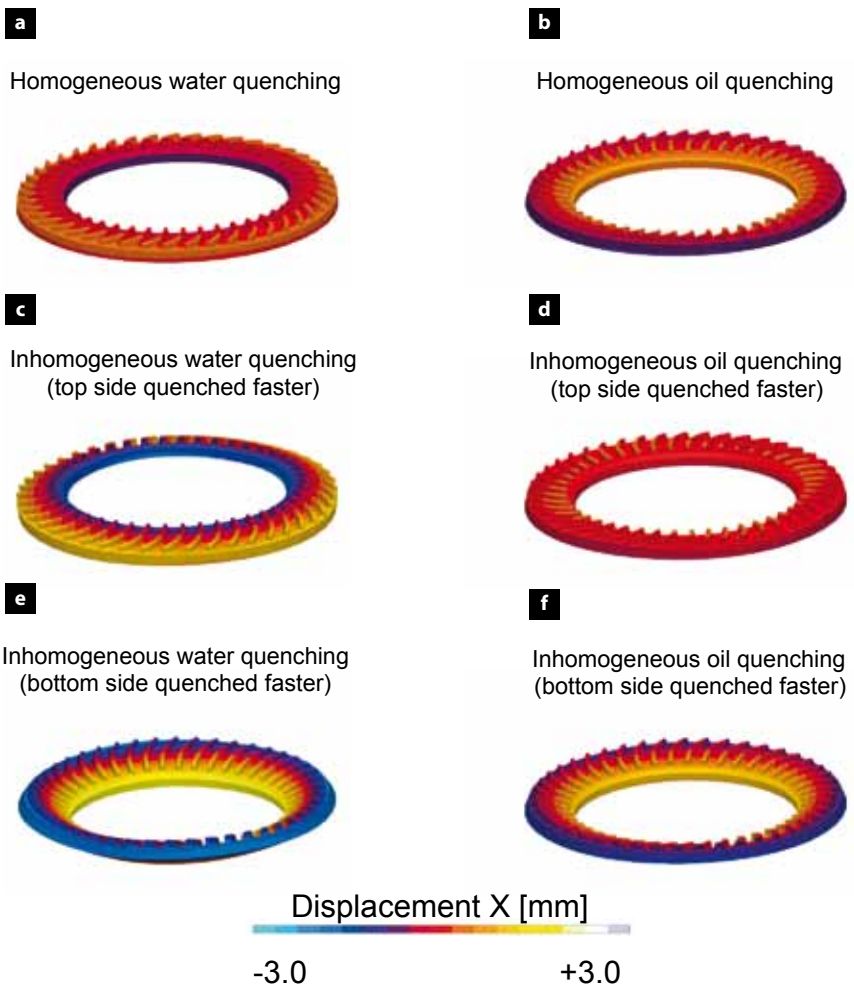

Figure 24: Displacement in x-direction for a brake disk for different quenching conditions (a-f) presented with a distortion factor of 15 (quenching from 900 °C to room temperature).

and inhomogeneous quenching, where faster quenching was assumed for either the top or the bottom side, has been investigated.

The results presented in Figure 24 show the displacement component normal to the surface of the disc with a magnification factor of 15 for the different quench conditions.

7.1 Water quenching

The inhomogeneous water quenching generated the highest level of displacement, which was found to be in the range of several millimeters. The worst case was for the fast quenching of the bottom side. The direction of out of plane deformation depends on which side was quenched fastest. The homogeneous water quenching gave a moderate displacement level of less than 2 millimeters.

7.2 Oil quenching

Generally, the oil quenched brake discs showed less tendency to displacement. Faster oil quenching from the top side delivered the best out of plane displacement result. During quenching, the brake disc was first bent in one direction and later in the other direction, with the result being a more or less flat profile at the end of the quenching process. The faster oil quenching of the bottom side showed a larger amount of displacement compared to both the homogeneous water and oil quenching.

The maximum out of plane displacement is summarized as a function of quench conditions and cooling rate in **Table 1**. The example shows how optimization can be used to successfully minimize the amount of out of plane displacement and improve the quality of the casting after heat treatment.

8 Integrated distortion control in casting and heat treatment

Today it is possible to simulate the entire sequence of process steps and evaluate stress levels and distortion after both, casting and heat treatment. During both processes, thermal contraction and expansion lead to stresses and deformation, due to cooling, heating and quenching. The final dimensions of a cast component are clearly the result of the combination of process steps sued in its production. Simulation allows consideration of dimensional requirements throughout the entire process chain. Industry uses this possibility to optimize the casting design and make sure that support frames provide sufficient stability at high temperature during heat treatment.

In this section a large steel turbine blade from the Czech foundry ZDAS was investigated, [D]. The dimensional tolerances were carefully analyzed for the casting process and the stress relaxation was analyzed for the heat treatment process. The blade is part of a Francis turbine, with a weight of 13.4 tons, where the weight of the feeders and gating system is 8 tons. The dimensions are 4.3 x 3.5 m. The alloy is a martensitic stainless steel, CA-6NM. After casting, the part is heat treated by quenching from 1020 °C and tempered at 600 °C. The geometry of the blade is shown in **Figure 25**a, and the liquidus to solidus result from the casting simulation in Figure 25b.

Results from the casting stress analysis were used to preshape the pattern to compensate for the thermal contraction and distortion built up during the casting process. Pre-shaping was done to the CAD geometry, by applying the negative deviation between the results from the first simulation and the target geometry. Based on the updated CAD design, a second simulation was performed and compared to the target geometry. This first iteration of pre-shaping the design showed an improvement in the comparison to the target geometry. In **Figure 26**a the deviation to the target geometry is shown for the

Table 1: Maximum out of plane displacement for different cooling conditions of the brake disk obtained by virtual Design of Experiments.

Rank	Quenching condition	Average cooling rate on the top surface of the casting between 900 °C and 100 °C, K/s	Maximum difference in displacements in x-direction, mm
1	inhomogeneous oil quenching (top side faster quenched)	2.0	1.0
2	homogeneous water quenching	14.8	1.7
3	homogeneous oil quenching	2.7	2.0
4	inhomogeneous oil quenching (bottom side faster quenched)	2.1	3.0
5	inhomogeneous water quenching (top side faster quenched)	8.0	3.8
6	inhomogeneous water quenching (bottom side faster quenched)	11.1	5.1

original simulation and in Figure 26b the deviations after simulating the pre-shaped design. The maximum deviation on both sides of the blade is reduced from around 22 mm to 6 mm. It was decided to use the modified CAD design to create a wooden pattern for casting the first blades.

Six castings were manufactured and the parts were 3D-measured on both sides to evaluate the deviation to the target geometry, which was then compared to the simulation results. One of the measurement results is shown in **Figure 27**. The numbers in the blue boxes are measurements and numbers in the green boxes are simulation results. It should be noted that 13 mm of machining allowance has been added to the simulation results in order to compare numbers to the measurements.

Comparing the simulation results to the measurements is quite challenging for this type of component, and the agreement depends on a careful positioning of the curved surfaces. Measurements of the six parts also showed some spread in the deformation between the real parts. For the selected comparison some overall agreement was found in bigger sections with only a few millimeters of difference, but in some sections a bigger difference was found in the range of 6-9 millimeters. Some of the bigger difference seems to be local fluctuations in the measurements and local deviations in the curvature, which is not predicted by the simulation. Nevertheless, the foundry found the agreement reasonable taking the complex geometry into account, which is generally known to be complicated to keep consistently within tolerances. With the help of pre-shaping the CAD design, they were able to manufacture the parts within the tolerances of the machining allowance and minimize repair welding.

The blades were positioned for the subsequent heat treatment process as shown in **Figure 28**a and finally they were prepared for the nondestructive testing as shown in Figure 28b.

The heat treatment process was analyzed to evaluate the level of stress relaxation at high temperature

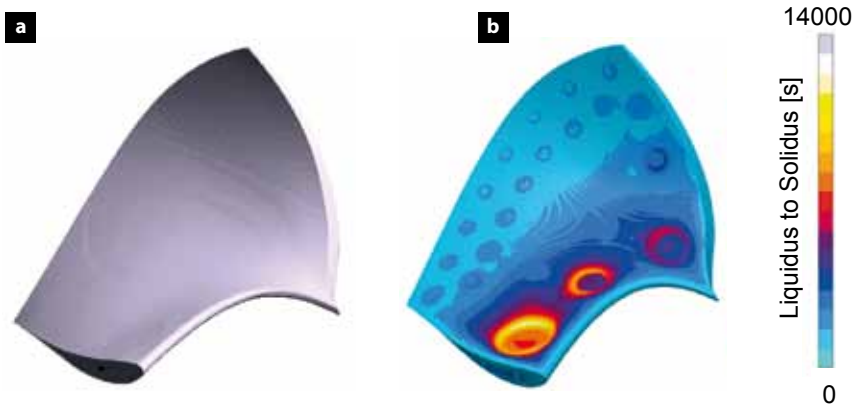

Figure 25: The geometry of the blade (a) and the liquidus to solidus result from the casting simulation (b).

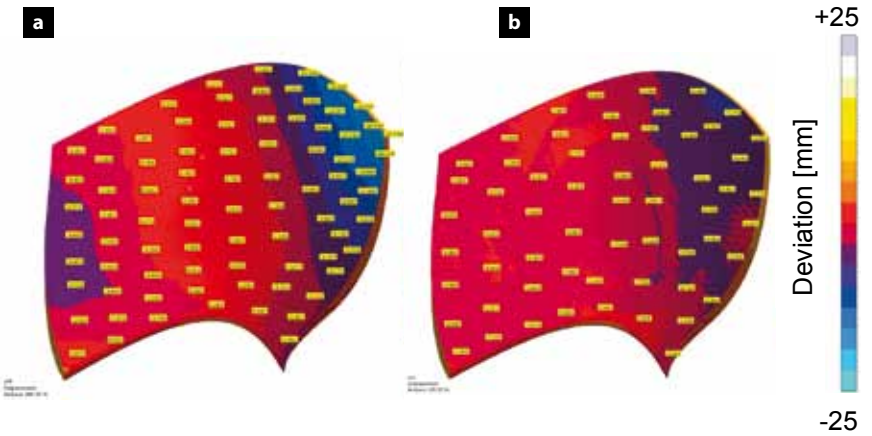

Figure 26: Deviation between the simulated distortion and the target geometry: Initial calculation (a) and after pre-shaping (b).

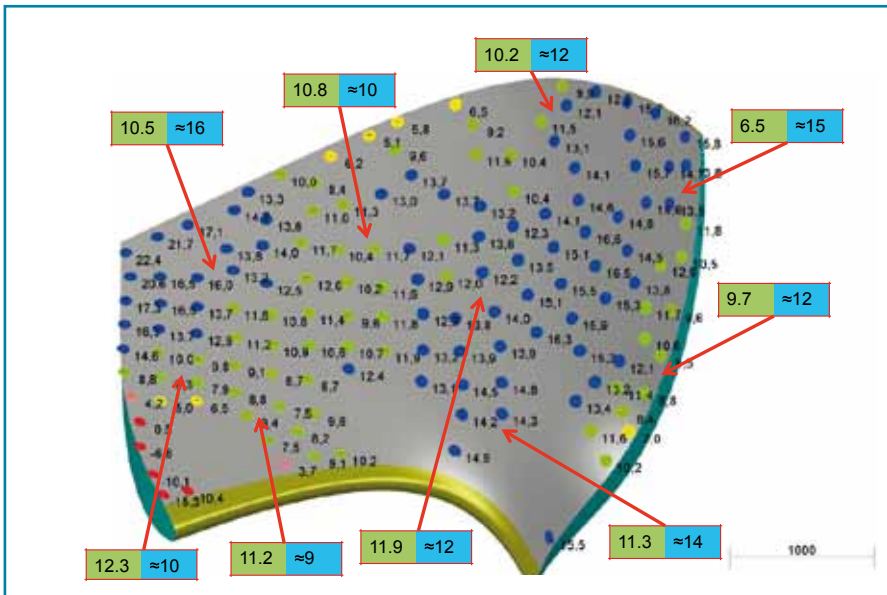

Figure 27: Deviation between production part and the target geometry. Numbers in green boxes are simulation results and numbers in blue boxes are measurements.

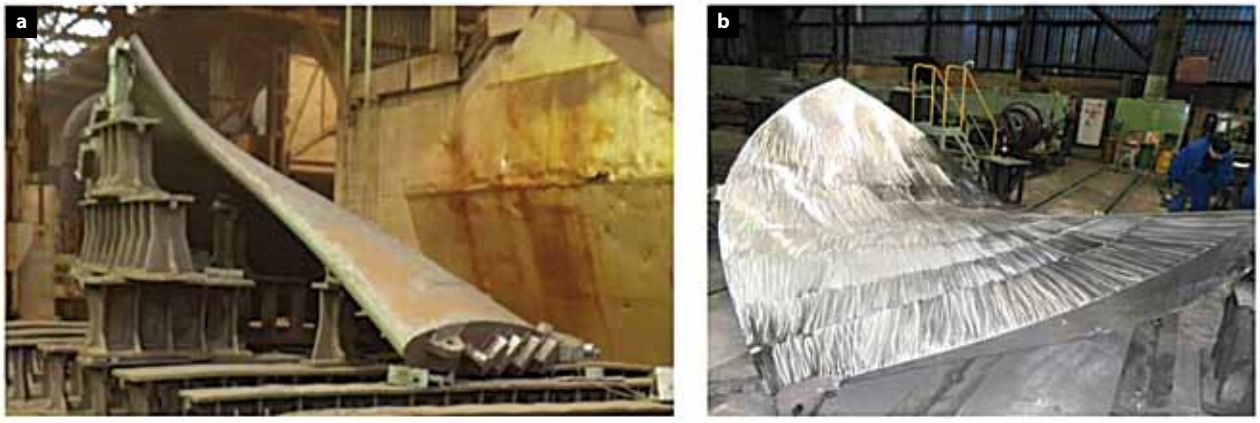

Figure 28: The blade positioned for heat treatment (a) and the blade after machining, being prepared for NDT (b).

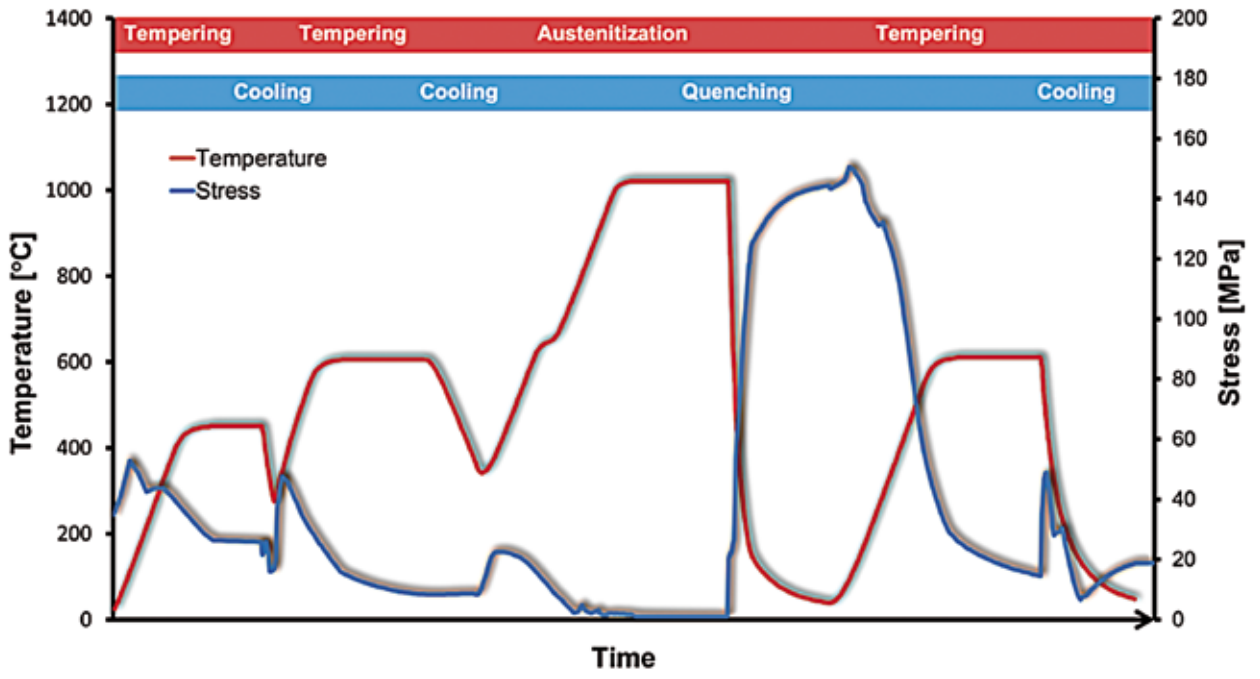

Figure 29: Temperature profile during heat treatment and the corresponding stress development in the interior part of the thick section of the blade.

and the building up of stresses during cooling and quenching. Furthermore, the change in shape was evaluated at the end of heat treatment by comparing the final distortion level to the shape after casting. The unified creep model was used to have a proper description of the time and temperature dependency, which governs the stress relaxation at high temperature in the furnace. To visualize the temperature and stress level in the blade a point was selected in the thick section. The two curves are shown in **Figure 29**.

The temperature and stress profile of the heat treatment process clearly indicates the expected stress relaxation at elevated temperature, followed by an increase in stress level during cooling. The stress level sensitivity to cooling rate and thermal gradients is seen by the big increase in stress level during quenching compared to the lower increase in stress level during the slower cooling steps.

The result in **Figure 30** shows the additional deformation, which was built up during the heat treatment steps. The comparison is based on a best fit approach and it indicates that the main downward deformation is localized in the upper thick region and some smaller upward deformation is localized in the center of the blade.

Overall, the stepwise analysis of the blade reduced the risk of producing blades outside of tolerances, which would require expensive repair welding and delays in production. Using the unified creep model to analyze the heat treatment process, it

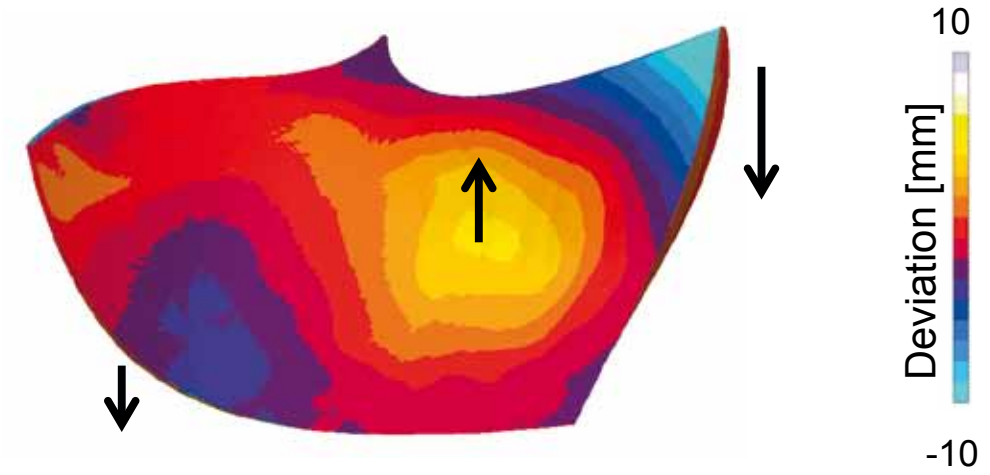

Figure 30: Deviation in shape from the as-cast state to the final heat treated state.

was possible to get an impression about the performance of the support structure and the development in the stress state during multiple heating and cooling cycles.

9 Summary

Today, stress simulation of sand casting and subsequent processes extends the possibility to identify critical regions in the part and evaluate dimensional requirements that influence the in-service performance. Validation of the applied models has shown reliable stress levels even for large, slow cooling parts where stress relaxation is taken into account. Integrating the results from the thermal analysis makes it possible to predict the risk of cracks at high and intermediate temperature levels such as hot tears. In combination with the capabilities using virtual Design of Experiments, stress simulations can be used to analyze the influence of various parameters on the final quality of the part, and the results can be used to optimize the product and process conditions. Using the results systematically provides a strong tool to reduce the need for weld repair and reduce the scrap rate due to crack related problems or dimensions being outside required tolerances.

Dr. Jesper Thorborg, Dipl.-Ing. Jörg Zimmermann, Dr.-Ing. Corinna Thomser, MAGMA GmbH, Aachen

Acknowledgements

[A] Material provided by MAN Energy Solutions, Denmark
[B] Material provided by WEG S.A., Brazil
[C] Material provided by Eagle Alloy, Inc., Muskegon, Michigan, USA
[D] Material provided by ŽĎAS, a.s., Czech Republic

Literature

[1] Anand, L: Constitutive equations for the rate-dependent deformation of metals at elevated temperatures. J. of Eng. Materials and Technology 104 (1982), pp 12-17.
[2] Chan, K. S., et. al.: A survey of unified constitutive theories. Second Symposium on Nonlinear Constitutive Relations for High Temperature Applications, NASA Lewis RC, 1984.
[3] Frost, J.; Ashby, F.: Deformation-mechanism maps: The plasticity and creep of metals and ceramics. Pergamon Press, 1982.
[4] Simo, J. C.: Computational inelasticity. Springer Verlag, New York, 1997.
[5] Thorborg, J.; Klinkhammer, J.; Heitzer, M.: Transient and residual stresses in large castings, taking time effects into account. Proc. from the 13th Int. Conf. on, Modeling of Casting, Welding and Advanced Solidification Processes. Vol. 13, eds. Ludwig, A.; Wu, M.; Kharicha, A. IOP Conf. Ser.: Mater. Sci. Eng. 33 (2012) 012050.